A PROBABILISTIC APPROACH FOR DYNAMIC FRAGMENTATION OF CERAMICS UNDER IMPACT LOADING

C. DENOUAL,[1] F. HILD[2] and C. COTTENOT[1]

[1]DGA / CREA – Département Matériaux en Conditions Sévères
16 bis, Avenue Prieur de la Cote d'Or, F–94114 Arcueil Cedex, France.

[2]Laboratoire de Mécanique et Technologie
E.N.S. de Cachan / C.N.R.S. / Université Paris 6
61, Avenue du Président Wilson, F–94235 Cachan Cedex, France.

ABSTRACT

Impact produces high stress waves leading to fragmentation of brittle materials such as ceramics. The main mechanism used to explain the size variation of fragments with stress rate is an obscuration phenomenon. When a flaw initiates, the released stresses around the crack prevent other nucleation in an increasing zone. After a presentation of a statistical approach, the evolution of the number of nucleated flaws is derived. Using a Weibull model, some numerical results and an analytical lower bound are proposed. The number of fragments is found to increase with the stress rate and the Weibull parameter.

KEYWORDS

Impact, dynamic loading, ceramic materials, fragmentation, statistical approach.

INTRODUCTION

Bilayered armor with ceramic as front plate and steel as back plate has been used for several years to improve the efficiency of light armor (den Reijer, 1991) or medium armor (Briales *et al.*, 1995). The high hardness of ceramic materials favors projectile failure (Orsini and Cottenot, 1995) and spreads the kinetic energy on a large surface of a ductile back face. The weight of the armor is then reduced in comparison to an armor made of steel only. In most impact configurations, the stress field associated with impact can be assumed to be spherical and an analogy can be made between real impact failure morphologies and soft recovery experiments of divergent spherical stress load (Tranchet, 1994). The first result is that stress waves can produce damage both in compressive and tension modes in two different locations in the ceramic (Fig. 1). Damage in compression is produced near the impact surface when shear stresses reach a threshold value which can be dependent on pressure and strain rate. In the bulk of the ceramic, damage in tension is observed when the hoop stress induced by the radial motion of the impacted ceramic is sufficiently large to generate fracture in mode I initiating on micro defects such as porosities or inclusions. With a projectile velocity under 1000 m/s, no significant perforation can be observed while damage grows. One can then uncouple the damage evolution phase from the complete penetration phase. The complete perforation is dependent on the way the ceramic fractures in terms of damage location and evolution, and in terms of anisotropic behavior due

to cracking. The present study deals with the generation of damage in ceramics due to the tensile stress state that follows the compressive stress wave induced by impact.

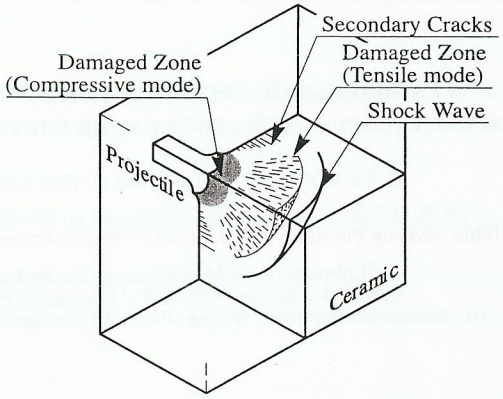

Fig. 1. Morphology of damage in a ceramic specimen during impact.

Orientation of cracks given by post–mortem observations (Tranchet, 1994) are consistent with a generation of damage by the tensile hoop stress state that follows the longitudinal compressive wave. Since most of the initiated cracks do not exceed a few millimeters, one can assume that the crack tip cannot follow the cracked front, i.e. the velocity of the former is less than the velocity of the latter. A crack initiates when the tensile stress reaches a threshold value (depending on the size and shape of the defect) and stops because of other defects nucleated in front of it. Damage generation can then be described as a local problem, depending on the local stress state.

FRAGMENTATION ANALYSIS

Many defects do not cause any cracks to nucleate during the increase of the tensile stress. In this paper a model of fragmentation in brittle materials is proposed. It takes into account exclusion phenomena based on an analysis of the way the stresses are released around a crack and obscure other defects. Since all the cracks nucleate only for an increasing tensile stress, decreasing or stationary global stresses will not be considered in further discussion. When a fracture initiates, the local stress state is modified by a concentration of shear stress near the crack tip and normal stress relaxation at the middle of the crack. In brittle materials such as ceramics, the velocity of the crack tip is not negligible with respect to the wave celerity and the zone affected by fracture is a complex function of time, crack velocity and stress wave celerity. To understand why a crack nucleates, one has to model the interaction of the stress affected volume and other defects that should nucleate. The behavior of a flaw around a nucleated one can be described by three different cases:

1 the flaw is far from the nucleated one and the stress state is not affected,

2 the flaw is in the affected volume but the local tensile stress still increases, i.e. initiation may occur,

3 the flaw is in the affected volume and the local tensile stress is decreasing, i.e. no crack is emanating from this potential initiation site.

To make the analysis tractable, only volumes defined by cases 1 and 3 will be considered, the volume defined by the case 2 is assumed to be insignificant in this problem. Furthermore, the stress state in the material is assumed to be homogeneous (i.e. the direction of the maximum principal stress is constant) which allows a unidimensional expression of tensile stresses. If the stress gradient is small, the space dimension can be uncoupled from the tensile stress (or time) dimension and flaw nucleation can be represented on a time – space graph (Fig. 2). The space location of the defects are represented in a simple abscissa (instead of a three–dimensional representation) of an x–y graph where the y–axis represents the time (or stress) to failure of a given defect. The first crack nucleation occurs at time T_1 (corresponding to a stress $\sigma[T_1]$) at the space location M_1 and produces an "obscured volume" $V_1(T)$ increasing with time. At time T_2 (corresponding to a stress $\sigma[T_2] > \sigma[T_1]$) a second defect nucleates in a non–affected zone and produces its own obscured volume. The third and fourth defects do not nucleate because they are obscured by the first and both first and second defects, respectively. The sum of all the obscured zone has been proposed by Kipp and Grady (1979) to define the volume in which no crack can occur. Because different obscured volumes may overlap (i.e. a flaw can be obscured by one or more other cracks), its preferable to define the conditions of non–obscuration for a given defect by examining the *reverse* problem. For a given flaw D a non–interaction zone can be defined in which a defect cannot obscure D (Fig. 3) and the interaction zone in which a defect will always obscure D.

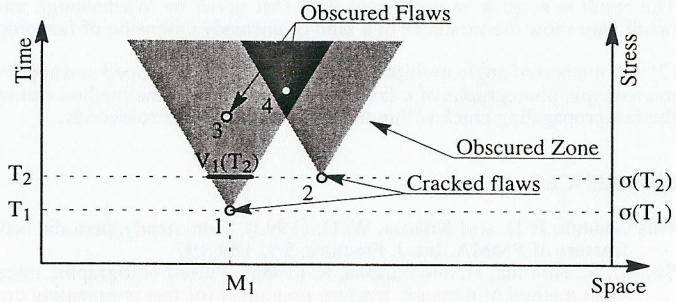

Fig. 2. Fragmentation and obscuration phenomena.

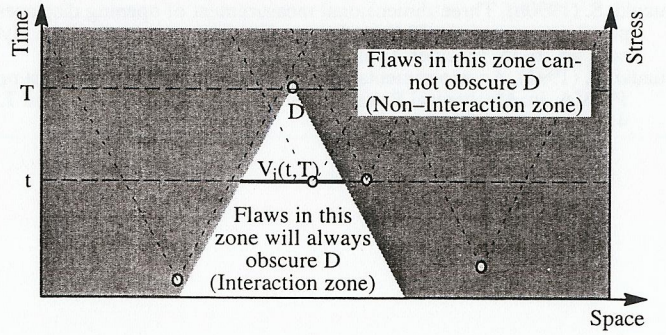

Fig. 3. Schematic of the interaction and non–interaction zones.

The flaw distribution can therefore be split into two parts and the average number of broken flaws can be written as

$$\mu_b(T,V) = \mu_T(T,V) - \mu_o(T,V) \tag{1}$$

where μ(T,V) denotes the mean number of flaws that may break in a volume V for a stress greater than or equal to σ(T). The subscripts indicate the effectively broken (b) flaws, the obscured flaws (o), and the total number of flaws (T). During a time (or stress) increase from T to T + ΔT, the number of broken flaws in a volume V will increase by $\Delta T \partial\mu_b(T,V)/\partial T$. New cracks will initiate only if the defect exists in the volume V and if no crack is broken in its interaction zone

$$\frac{\partial\mu_b(T,V)}{\partial T} = \frac{\partial\mu_T(T,V)}{\partial T} P_{no}(T) \tag{2}$$

where P_{no} is the probability that no defect was broken in the interaction zone. The probability of non–interaction can be split in an infinity of *independent events* of probability $\Delta P_{no}(t)$ defined during a time (or stress) increment ΔT. With a small time increment, $\Delta P_{no}(t)$ is defined as follows

$$\Delta P_{no}(t) \approx 1 - \frac{1}{V}\frac{\partial\mu_b(t,V)}{\partial t} V_i(t,T)\Delta T \quad with \quad t \le T \tag{3}$$

where V_i(t, T) the interaction volume at t for a defect that should break at T. Thus P_{no} is given by

$$P_{no}(T) = \prod_{t=0}^{T} \Delta P_{no}(t) \tag{4}$$

$$P_{no}(T) = Exp\left[\sum_{t=0}^{T} ln\left(1 - \frac{\partial\mu_b(t,V)}{\partial t}\frac{V_i(t,T)}{V}\Delta T\right)\right] \tag{5}$$

$$P_{no}(T) \approx Exp\left[\int_0^T -\frac{\partial\mu_b(t,V)}{\partial t}\frac{V_i(t,T)}{V}dt\right] \tag{6}$$

The evolution of μ_b (T, V) can now be expressed as the solution of a differential equation

$$\frac{\partial\mu_b(T,V)}{\partial T} = \frac{\partial\mu_T(T,V)}{\partial T} Exp\left[-\int_0^T \frac{\partial\mu_b(t,V)}{\partial t}\frac{V_i(t,T)}{V}dt\right] \quad with \quad \begin{cases}\mu_b(T=0,V)=0\\ \mu_T(T=0,V)=0\end{cases} \tag{7}$$

If the brittle material is homogeneous, the μ(T,V) variables can be written as follows

$$\mu(T,V) = V\lambda(T) \tag{8}$$

where λ(T) is the mean number of nucleated flaws per unit volume. In order to make Eqn. (7) dimensionless, new definitions of time, interaction volume and mean number of nucleated flaws per unit volume are chosen (the subscript "c" denotes characteristic values of variables)

$$\bar{t} = \frac{t}{t_c} \;;\; \overline{\lambda_b}(t) = \frac{\lambda_b(t)}{\lambda_c} \;;\; \overline{\lambda_T}(t) = \frac{\lambda_T(t)}{\lambda_c} \;;\; \overline{V_i}(t,T) = \frac{V_i(t,T)}{V_{ic}} \tag{9}$$

$$\lambda_c V_{ic} = 1 \tag{10}$$

The characteristic density $\lambda_c = \lambda_T(t_c)$ and volume $V_{ic} = V_i(0, t_c)$ are both defined from t_c which can be described as the time for which one defect is broken in a volume equal to the interaction volume (see Eqn. (10)). The dimensionless differential equation can then be obtained using Eqns. (7–10)

$$\frac{d\overline{\lambda_b}(\bar{T})}{d\bar{T}} = \frac{d\overline{\lambda_T}(\bar{T})}{d\bar{T}} Exp\left[-\int_0^{\bar{T}} \frac{d\overline{\lambda_b}(\bar{t})}{d\bar{t}}\overline{V_i}(\bar{t},\bar{T})d\bar{t}\right] \quad with \quad \begin{cases}\overline{\lambda_b}(\bar{T}=0)=0\\ \overline{\lambda_T}(\bar{T}=0)=0\end{cases} \tag{11}$$

At the beginning of the loading, no interaction occurs and therefore $\overline{\lambda_b}(\bar{T}) \approx \overline{\lambda_T}(\bar{T})$ and as more and more defects nucleate $\overline{\lambda_b}(\bar{T}) \ll \overline{\lambda_T}(\bar{T})$. It is expected that the number of broken flaws saturates when $\bar{T} \to \infty$ even though the total number of flaws may approach infinity.

APPLICATIONS

The static description of brittle materials can be given by a two–parameter Weibull model. The mean number of flaws per unit volume is then assumed to follow a power law function

$$\lambda_T(\sigma) = \frac{1}{V_o}\left(\frac{\sigma}{S_o}\right)^m \tag{12}$$

where m is the Weibull modulus and S_o the scale parameter relative to a volume V_o.

One can notice that if the interaction volume is equal to the entire volume of the structure (i.e. the loading rate is very small and the ratio $V_i/V = 1$), $P_{no}(T)$ defined by Eqn. (6) is equivalent to the probability that no flaw will break in a constant volume V for a stress less than or equal to σ(T). Eqn. (6) can then be expressed as

$$P_{no}(T) = Exp\left[-\mu_b(T,V)\right] \tag{13}$$

and is equal to the probability of finding zero critical flaws in a volume V (i.e. $P[N_b(T,V) = 0]$). This result is in accordance with a Poisson model describing the probability of finding n broken flaws in a volume V

$$P[N_b(T,V) = n] = \frac{\left[\mu_b(T,V)\right]^n}{n!} Exp\left[-\mu_b(T,V)\right] \tag{14}$$

The probability of non–interaction becomes the complement of the failure probability $P_f = 1 - P[N_b(T,V) = 0]$ which can be modeled by a classical Weibull law

$$P_f = 1 - Exp\left[-\frac{V}{V_o}\left(\frac{\sigma}{S_o}\right)^m\right] \tag{15}$$

Usually, the interaction volume cannot be assumed as a time–constant variable and since no analytical expressions are available for V_i, an approximation will be proposed.

Both experimental and analytical approaches show that the velocity of cracks in brittle materials rapidly reaches a constant value depending on mechanical parameters such as the longitudinal wave celerity and Poisson's ratio (Bluhm, 1969 ; Freund, 1972). Some approximations can then be made on the interaction volume V_i(t,T) to make the following calculus easier. First, the shape of V_i is supposed to be constant, i.e. all the interaction volumes are self–similar and can be written as

$$V_i(t,T) = S\left[L_c(T-t)\right]^3 \tag{16}$$

where S is a shape parameter, L_c(T–t) is a characteristic length which is a function of the crack propagation time T – t. Second, L_c is assumed to be linear with the crack length, i.e. it can be written as proportional to the sound velocity. The time evolution of V_i can therefore be taken as

$$V_i(t,T) = Sk^3C^3(T-t)^3 \;\;;\;\; 0 \le t \le T \tag{17}$$

where k is a real number varying within the range [0 ; 1], C is the longitudinal stress wave velocity and kC(T–t) the characteristic length function. In the following, only dynamic loadings will be considered with a stress rate $d\sigma/dt = \dot{\sigma}$ assumed to be constant. Eqn. (12) becomes

$$\lambda_T(T) = \frac{\dot{\sigma}^m}{V_o S_o^m} T^m \quad and \quad \overline{\lambda_T}(\bar{T}) = \bar{T}^m \tag{18}$$

The characteristic time t_c can now be expressed by solving Eqn. (10)

$$t_c = \left(\frac{\dot{\sigma}^m}{V_o S_o^m} S k^3 C^3 \right)^{-\frac{1}{m+3}} \tag{19}$$

The dimensionless differential equation can be rewritten as

$$\frac{d\overline{\lambda_b}(\overline{T})}{d\overline{T}} = m\overline{T}^{m-1} Exp\left[- \int_0^{\overline{T}} \frac{d\overline{\lambda_b}(\bar{t})}{d\bar{t}} (\overline{T} - \bar{t})^3 d\bar{t} \right] \quad with \quad \overline{\lambda_b}(\overline{T} = 0) = 0 \tag{20}$$

No analytical solutions can be proposed for this equation and numerical simulations have to be used. In all the results presented in Fig. 4., the dimensionless number of nucleated defects reaches a maximum value which is *only* dependent on the Weibull modulus. This result can be shown by analyzing Eqn. (20). The saturation phenomenon is consistent with the description of the nucleation mechanism which is given as a competition between nucleation of defects and stress release. The fragmentation process saturates when all the stresses are released in the structure, i.e. no defect can break anymore.

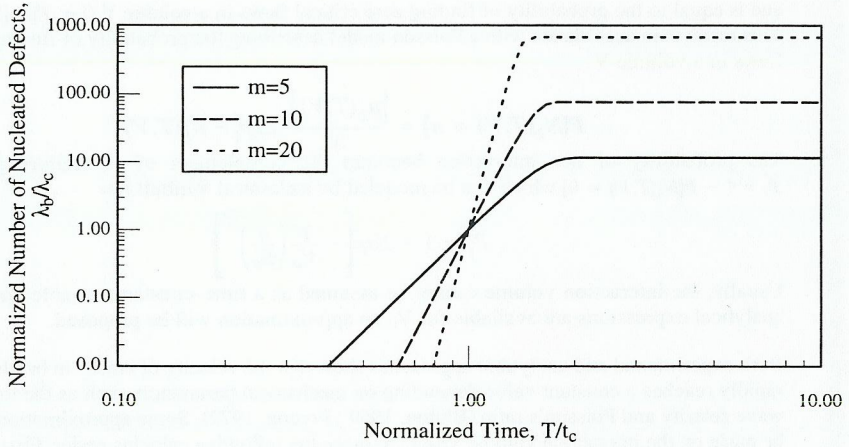

Fig. 4. Numerical simulations of number of broken flaws as a function of time for three different Weibull moduli m.

Furthermore, one can observe that the number of nucleated flaws increases with the Weibull modulus. An explanation to this phenomenon can proposed using Eqn. (12). With a high Weibull modulus m, the number of defects will increase dramatically in a small time step when the stress becomes greater than S_o. Because of the time dependence of the saturation mechanism, many defects nucleate before any significant saturation and the material will be fully fragmented. If m is small, there is much more time between two crack initiations. The first nucleated defects can then obscure others before their own nucleation and only few defects eventually nucleate.

To give a lower bound to the numerical results, the number of nucleated defects cannot be greater than the number of initial defects (see Eqn. (11))

$$\lambda_b(T) \leq \lambda_T(T) \tag{21}$$

Therefore a lower bound to the increment of broken defects can be obtained

$$\frac{d\overline{\lambda_b}(\overline{T})}{d\overline{T}} \geq m\overline{T}^{m-1} Exp\left[\frac{-6\overline{T}^{m+3}}{(m+1)(m+2)(m+3)} \right] \tag{22}$$

The dimensionless lower bound to the number of broken flaws at saturation can be derived and is *only* dependent on the Weibull modulus m

$$\overline{\lambda_b}(\infty) \geq \frac{m}{m+3} \left[\frac{(m+1)(m+2)(m+3)}{6} \right]^{\frac{m}{m+3}} \Gamma\left(\frac{m}{m+3} \right) \tag{23}$$

where Γ is the Euler function of the second kind. A comparison between numerical results and the lower bound is given in Fig. 5.

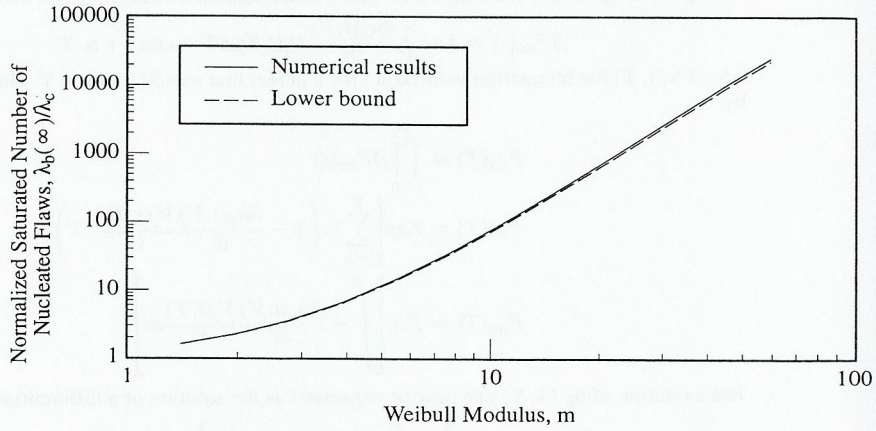

Fig. 5. Evolution of the normalized saturated number of broken flaws as a function of the Weibull modulus.

The difference between the lower bound and the numerical simulations does not exceed 10% in the range [2 ; 60]. The complete result can be written using Eqns. (10, 17, 18, 23)

$$\lambda_b(\infty) \geq f(m) \left(\frac{\dot{\sigma}^m}{V_o S_o^m} \right)^{\frac{3}{m+3}} \left(S k^3 C^3 \right)^{-\frac{m}{m+3}} \tag{24}$$

$$with \quad f(m) = \frac{m}{m+3} \left[\frac{(m+1)(m+2)(m+3)}{6} \right]^{\frac{m}{m+3}} \Gamma\left(\frac{m}{m+3} \right)$$

The number of broken flaws at saturation is proportional to a power function of the stress rate $\dot{\sigma}$. This result can be compared to the one obtained by Grady (1982). In his approach, the fragmentation size is controlled by the competition of the energy created by the fragment surface and the use of local kinetic energy. Assuming that all the fragments have the same diameter d, Grady shows that

$$d = \left[\frac{\sqrt{20} K_{IC}}{\rho C \dot{\epsilon}} \right]^{2/3} \propto \dot{\epsilon}^{-2/3} \tag{25}$$

where K_{IC} denotes the fracture toughness, C the sound velocity in the solid, $\dot{\epsilon}$ the linear strain

rate and ρ the material density. Equation (25) was successfully applied to predict the stress rate dependence of the fragment size of oil shale. The diameter d can also be written using the density $\lambda_b(\infty)$ representing the average number of nucleated flaws equal to the number of fragments

$$d = \left[\lambda_b(\infty)\right]^{-1/3} \propto (\dot{\sigma})^{\frac{-m}{m+3}} \tag{26}$$

Because of linearity, the evolution of the fragment diameter according to stress or strain rate can then be comparable for the above mentioned approaches if the Weibull modulus is equal to 6 (i.e. m/(m+3) = 2/3) which is an acceptable value for oil shale (Kipp and Grady, 1978).

CONCLUSIONS

A statistical approach has been proposed to describe the stress rate dependence of the fragmentation mechanism. The saturation phenomenon is illustrated by numerical results and leads to a prediction of the total number of broken flaws. An analytical lower bound is obtained and represents a good approximation of the exact solution. The latter is useful to describe the evolution of broken flaws with the material parameters. The proposed approach can be used to develop a damage evolution law in tensile mode for impact simulations on ceramics.

ACKNOWLEDGMENT

This work was supported by DGA/DRET/STRDT (General Delegation for Armament, Direction of Research and Technology, Technical Service of Research and Technological Development).

REFERENCES

Bluhm, J. I. (1969). Fracture Arrest. In: *Fracture* (H. Liebowitz, ed.), Vol. V, pp. 1–63. Academic Press, New York.

Briales, C., R. Cortés, R. Zeara, M. A. Martínez and V. Sánchez–Gálvez (1995). An experimental and numerical study on the impact of ballistic projectiles onto ceramic/metal armours. In: Proc. 15th Int. Symp. on Ballistics, Jerusalem, pp. 19–26.

den Reijer, P. C. (1991). Impact on ceramic faced armour, PhD dissertation, Delft Technical University, The Netherlands.

Freund, L. B. (1972). Crack propagation in an elastic solid subjected to general loading- Constant rate of extension. *J. Mech. Phys. Solids*, **20**, pp. 129–140.

Grady, D. E. (1982). Local inertial effects in dynamic fragmentation. *J. Appl. Phys.* **53** (1), pp. 322–325.

Kipp, M. E. and Grady, D. E. (1979). Numerical studies of rock fragmentation. SAND79–1582 Report . Sandia National Laboratoties, Albuquerque, NM.

Orsini, H. and C. E. Cottenot (1995). Specific test to evaluate intrinsic ballistic properties of ceramic materials against an AP 12.7 mm projectile. Application to improve ceramic materials. In: Proc. 15th Int. Symp. on Ballistics, Jerusalem, pp. 183–190.

Tranchet, J. Y. (1994). Comportement de deux matériaux fragiles polycritallins sous l'effet de la propagation d'une onde sphérique divergente. PhD Dissertation, University of Bordeaux I.